Coordinated Active Steering and Four-wheel Independently Driving/Braking Control with Control Allocation – A Review

Pradeep Gopal and Sahana Anbazhagan

As part of coursework for Control of Robotic Systems, University of Maryland, College Park

***Abstract* - This paper presents a detailed review of the theoretical aspects of the chosen research paper [1]. A hierarchical coordinated control algorithm for integrating active front steering and four-wheel independently driving/braking control is studied. An adaptive sliding mode control law and a coordination law is chosen for the higher-level controller to adjust the yaw rate and slip angles. Control priorities are applied to determine the desired front wheel steering angle and external yaw moment. Actuators and tire forces constraints are taken into consideration to assign the desired yaw moment to the front wheel steering system and four wheels. This is achieved by using a control allocation algorithm for a lower level controller. The vehicle stability index provides the weighting factors and control inputs in the cost function which are updated online. The paper then presents the results of simulations that verifies the stability and handling of the vehicle getting improved with the proposed controller and more control to sideslip angle is made possible while the vehicle is hitting the maneuvering limitations.**

I. INTRODUCTION

Vehicles employing four in-wheel motors to directly actuate its four wheels, without any mechanical links, such as transmissions or differentials are found to provide higher efficiency in terms of performance and stability [2]. The torque as well as driving/braking mode of each wheel can be controlled independently. Such actuation flexibility together with the electric motors' fast and precise torque responses not only can enhance vehicle motion/stability control performance [3], [4], [5] but also offer new avenues for improving the vehicle's operational energy efficiency. Compared to mechanical drivetrains, electric ground vehicles that are driven by four independently actuated in-wheel motors have better performance in terms of stability and energy efficiency. But stability maintenance during critical driving and behavior during normal driving is better in case of the steer-by-wire systems which uses electrical or electro-mechanical systems for performing vehicle functions traditionally achieved by mechanical linkages in comparison to the traditional steering system.

Considering the consumption of motor energy, a combination active steering and four-wheel independently driving/braking system offers a better performance. A multi – layer control architecture is more effective and flexible for coordinating vehicle subsystems [6]. Using this architecture, the higher-level controller calculates the global control efforts of desired yaw moment and Active steering control is effective for improving vehicle characteristics and maintaining the vehicle stability by generating an opposite yaw moment near the limitation of tire road adhesion by reducing the steering angle. But when the vehicle is very close to the handling limit, active steering control becomes inefficient in following the desired yaw rate. Results show that, Variable Torque Distribution (VTD) has effects on yaw moment and acceleration. In case of handling limit, Brake Force Distribution (BFD) including differential braking are more effective than Active Front-Wheel Steering (AWS) and VTD in tracking yaw rate and bounding sideslip [7].

The main advantage of control allocation is the capability of using multiple control objectives and constraints of actuators. Also, reconfigurability during failure of actuators and maximizing the potential of tire forces. The optimization-based allocation techniques used theoretically has weightings of multiple control objectives kept pre-set and constant throughout the maneuvering scenarios. However, practically the importance of tracking the desired yaw moment and maintaining the stability will impact the vehicle state changes like criticality of stability.

In this paper, they have applied hierarchical control structure. In order to determine the desired front wheel steering angle and the desired yaw moment in the higher-level controller, an adaptive sliding mode control law and a coordination weighting law have been applied. While, in lower level controller in order to allocate the desired control signals to each other, a control allocation method with input saturations and rate limit considerations have been implemented. The factors for tracking the error and the control inputs in the cost function are updated on a real time basis, online, based on the proposed stability index.

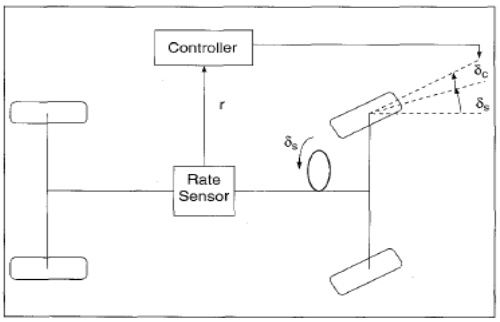

Fig. 1. Active steering phenomenon

II. SYSTEM MODELLING

A. Vehicle Model

Active Steering describes a steering system for a vehicle in which the relationship between the driver's steering inputs and the angle of the steered road wheels may be continuously and intelligently altered. It incorporates a power electric variable gear ratio power steering technology introduced by BMW in 2003 first appearing on the redesigned 5 Series which varies the degree that the wheels turn in response to the steering wheel [8]. At lower speeds, this technology reduces the amount that the steering wheel must be turned – improving performance in situations such as parking and other urban area traffic maneuvers. At higher speeds, the performance is such that the normal increased responsiveness from speed is avoided and it provides improved directional stability. The plant input is the front wheel steering angle (δ_f). In the active steering system of Fig. 1, it is composed of a conventional steering angle (δ_s), commanded by the driver and an additive steering angle (δ_c), generated by the feedback controller, such that

$$\delta_F = \delta_s + \delta_c$$

For robust unilateral decoupling δ_c must compensate the influence of yaw rate on Lateral force. The Active Front Steering (AFS) can also be used in yaw rate control and have been confirmed very effective in small and medium lateral acceleration condition [8]. However, when the vehicle state is hitting the manoeuvring limitation, AFS may become inefficient in tracking the yaw rate. Although AFS is still available to achieve some contra-cornering yaw moment, restricting the side slip angle from being uncontrollable, it is not able to regulate β back to zero when the lateral acceleration is around its limitation

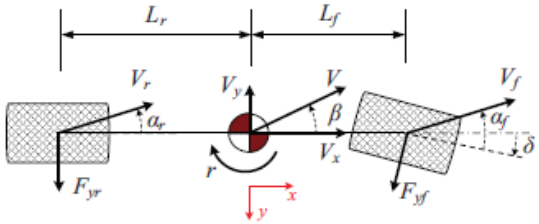

Fig. 2. A 2 DOF Vehicle Model

Considering all the tires have the same steering and slip angles, the vehicle lateral plane motion can be represented with a bicycle vehicle model which can be represented as [10],

$$\begin{cases} \dot{\beta} = \left(\frac{-2(C_f + C_r)}{mV_x}\right)\beta + \left(\frac{2(C_fL_f - C_rL_r)}{mV_x^2} + 1\right)r \\ \qquad + \left(\frac{2C_f}{mV_x}\right)\delta + d_1 \\ \dot{r} = \left(\frac{2(C_rL_r - C_fL_f)}{I_z}\right)\beta - \left(\frac{2(C_rL_r^2 + C_fL_f^2)}{I_zV_x}\right) \\ \qquad + \left(\frac{2C_fL_f}{I_z}\right)\delta + \left(\frac{M_{zc}}{I_z}\right) + d_2 \end{cases} \quad (1)$$

where, I_z is the vehicle inertia along the z-axis

r is the yaw rate

β is the vehicle sideslip angle

C_f and C_r are the values of the front and rear tire cornering stiffness respectively

d_1 and d_2 are the external disturbances

M_{zc} is the external yaw moment generated by the tire force difference between the two sides of the vehicle. It can be defined as

$$M_{zc} = \frac{l_s}{2}(F_{xfl} - F_{xfr} + F_{xrl} - F_{xrr})$$

where, l_s is the track width.

Considering, $M_z = M_{zc} + 2C_fL_f$

$$M_{zc} = M_z - 2C_fL_f\delta$$

$$\frac{M_{zc}}{I_z} = \frac{M_z}{I_z} - \frac{2C_fL_f\delta}{I_z}$$

Substituting this in (1),

$$\begin{cases} \dot{\beta} = \left(\frac{-2(C_f + C_r)}{mV_x}\right)\beta + \left(\frac{2(C_fL_f - C_rL_r)}{mV_x^2} + 1\right)r \\ \qquad + \left(\frac{2C_f}{mV_x}\right)\delta + d_1 \\ \dot{r} = \left(\frac{2(C_rL_r - C_fL_f)}{I_z}\right)\beta - \left(\frac{2(C_rL_r^2 + C_fL_f^2)}{I_zV_x}\right) \\ \quad + \left(\frac{2C_fL_f}{I_z}\right)\delta + \left(\frac{M_z}{I_z} - \frac{2C_fL_f\delta}{I_z}\right) + + d_2 \end{cases}$$

where,

$2C_fL_f\delta$ is the yaw moment induced by the front wheel steering angle δ.

From the above data, the vehicle model can be rewritten as

$$\dot{x} = Ax + Bu + d \quad (2)$$

where,

$$x = \begin{bmatrix}\beta \\ r\end{bmatrix}, u = \begin{bmatrix}\delta \\ M_z\end{bmatrix}, d = \begin{bmatrix}d_1 \\ d_2\end{bmatrix},$$

$$A = \begin{bmatrix} \left(\frac{-2(C_f + C_r)}{mV_x}\right) & \left(\frac{2(C_rL_r - C_fL_f)}{mV_x^2} - 1\right) \\ \left(\frac{2(C_rL_r - C_fL_f)}{I_z}\right) & \left(\frac{-2(C_rL_r^2 + C_fL_f^2)}{I_zV_x}\right) \end{bmatrix},$$

$$B = \begin{bmatrix} \left(\frac{2C_f}{mV_x}\right) & 0 \\ 0 & \frac{1}{I_z} \end{bmatrix}$$

Substituting the values for A, B, C and D in the state space equation (2) of the system is given by,

$$\dot{x} = \begin{bmatrix} \left(\frac{-2(C_f + C_r)}{mV_x}\right) & \left(\frac{2(C_rL_r - C_fL_f)}{mV_x^2} - 1\right) \\ \left(\frac{2(C_rL_r - C_fL_f)}{I_z}\right) & \left(\frac{-2(C_rL_r{}^2 + C_fL_f{}^2)}{I_zV_x}\right) \end{bmatrix} \begin{bmatrix} \beta \\ r \end{bmatrix} + \begin{bmatrix} \left(\frac{2C_f}{mV_x}\right) & 0 \\ 0 & \frac{1}{I_z} \end{bmatrix} \begin{bmatrix} \delta \\ M_z \end{bmatrix} + \begin{bmatrix} d_1 \\ d_2 \end{bmatrix}$$

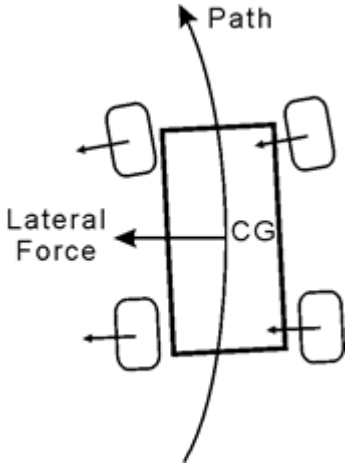

Fig. 3. Lateral Force on a curved path

III. SLIDING MODE CONTROLLER

A. *Reference Generation*

The controller is designed such that the desired yaw rate is tracked with the upper bound while restraining the vehicle side slip angle within tolerable limits. The desired steady state gain from the driver steering input to the yaw rate response can be obtained as,

$$G_{ss}(V_x) = \frac{V_x}{L + m\frac{C_rL_r - C_fL_f}{2}} \tag{3}$$

Then the desired yaw rate can be given by an empirical prefilter transfer function [3] as,

$$r_{des} = \frac{G_{ss}(V_x)}{0.1s + 1}\delta_d \tag{4}$$

From Fig. 2, the lateral acceleration at the centre of gravity of the vehicle can be given by,

$$a_y = V_x r + \dot{V}_y$$

$$= V_x r + \dot{V}_x \tan\beta + \frac{V_x\dot{\beta}}{\sqrt{1 + tan^2\beta}} \tag{5}$$

The lateral acceleration must be bounded by the maximum lateral force provided by the four wheels. Lateral forces can be easily understood as the forces acting in horizontal direction with respect to the plane of reference from Fig. 3. If the tire–road friction coefficient of each wheel is equivalent, the maximum resultant acceleration afforded by the tire forces is mg. When the longitudinal acceleration cannot be neglected, according to the 3-DOF vehicle model, the lateral acceleration must be constrained by,

$$a_y \leq \sqrt{\mu^2 g^2 - a_x^2} \tag{6}$$

where $a_x = \dot{V}_x - V_y r$. Further, if the side-slip angle of the vehicle and its derivative are both assumed to be small (i.e. the vehicle is assumed to be stable), the first term in (5) dominates, and the rest of the terms contribute a relatively small fraction of the total lateral acceleration. Hence, by combining equations (5) and (6) the upper bound of yaw rate can be given as,

$$r_{limit} = (1 - \theta)\sqrt{\frac{\mu^2 g^2 - a_x^2}{V_x}} \tag{7}$$

where θ is a positive constant, used to denote the contribution of the second and third terms of equation (5). Thus, by summing the above, the control target of yaw rate tracking is given by,

$$r_{target} = \begin{cases} r_{des}, & |r_{des}| < r_{limit} \\ r_{limit}sgn(r_{des}), & |r_{des}| \geq r_{limit} \end{cases} \tag{8}$$

and then, by substituting equation (8) into equation (5), the target value of the lateral acceleration is obtained as,

$$a_{y\_target} = V_x r_{target} + \dot{V}_y \tag{10}$$

The vehicle side-slip angle must also have an upper bound to ensure handling stability, with the empirical relation

$$|\beta| < \beta_{limit,}$$

$$\beta_{limit} = 0.02\mu g \tag{11}$$

This agrees with the desirable upper bound of slip angle on both high and low friction coefficient road [11]

B. *Adaptive Sliding Mode Controller Design*

Nonlinear control theory covers a wider class of systems that do not obey the superposition principle. It applies to more real-world systems, because all real control systems are nonlinear. The vehicle system, a real-world system is an intrinsic highly nonlinear system and linear controllers cannot account for all

the uncertainties existing in a real-world system. In order to provide more robust results taking into consideration all the disturbances and parametric uncertainties, an adaptive sliding mode controller is designed to calculate the desired yaw moment and front wheel steering angle. Sliding mode control, nonlinear control method alters the dynamics of a nonlinear system by application of a discontinuous control signal that forces the system to "slide" along a cross-section of the system's normal behavior [9].

The feedback control given to the system is not a continuous function of time and it switches from one continuous structure to another based on the current state space position. The trajectories always move towards an adjacent region with a different control structure and so the trajectory is not bounded entirely within one control structure. Instead, it slides along the boundaries of the control structure. The motion of the system as it slides along these boundaries is called a sliding mode and the geometrical locus consisting of the boundaries is called the sliding surface. For this system, the sliding mode surface is defined as,

$$s = x - x_{tg} \tag{12}$$

Where,

$x_{tg} = \begin{bmatrix} r_{tg} & \beta_{tg} \end{bmatrix}^T$

β_{tg}- vehicle slip angle reference

The reaching law of the sliding mode control for this system is given as,

$$\dot{s} = -\Lambda s - H\dot{s} - K(t)sign(s) + d \tag{13}$$

Where,

$\Lambda = diag(\lambda_1, \lambda_2)$

$H = diag(\eta_1, \eta_2)$

$K = diag(k_1, k_2)$

These positive definite matrices take care of the stability of the sliding mode control system. This can be proved by using a Lyapunov function. There are various types of stability tests, for the solutions of differential equations describing dynamical systems. The most important type is that concerning the stability of solutions near to a point of equilibrium. This may be discussed by the theory of Aleksandr Lyapunov. In simple terms, if the solutions that start out near an equilibrium point and if tends to stay near the equilibrium point forever, then the system can be proved to be globally stable [12].

Consider,

$$V = s^T s \tag{14}$$

Evaluating the time derivative of (14), we have

$$\dot{V} = s^T \dot{s} \tag{15}$$

Equation (13) can be simplified as,

$$\dot{s} + H\dot{s} = -\Lambda s - K(t)sign(s) + d$$

$$\dot{s}(I + H) = -\Lambda s - K(t)sign(s) + d$$

$$\dot{s} = (I + H)^{-1}(-\Lambda s - K(t)sign(s) + d) \tag{16}$$

Substituting for $\dot{s}$ from (16) in (15), we get

$$\dot{V} = s^T(I + H)^{-1}(-\Lambda s - K(t)sign(s) + d)$$

$$\dot{V} = -(I + H)^{-1}(-\Lambda s^T s + K(t)s^T sign(s) - s^T d) \tag{17}$$

We know that,

$(I + H) = diag(1 + \eta_1 1+, \eta_2)$ is positive definite, hence $(I + H)^{-1}$ is also positive definite

$s \neq 0$ and the disturbance is upper bounded, then $s^T s > 0$ and $s^T sign(s) > 0$

$K(t)$ chosen to be large, then $K(t)s^T sign(s) > s^T d$

Hence, $\dot{V} < 0$ and thus, the sliding mode control system is stable by the considered Lyapunov's rule.

The reaching law of the sliding mode control is given by,

$$\dot{s} = -\Lambda s - H\dot{s} - K(t)sign(s)$$

There is chattering due to the change of structural parameters and external disturbances. In order to eliminate these chattering, the $sign(s)$ with the saturation function $sat(E^{-1}s)$.

$$\dot{s} = -\Lambda s - H\dot{s} - K(t)sat(E^{-1}s)$$

Where,

Λ - defines the converge speed of s

$H\dot{s}$ – is applied to reduce the overshoot of the tracking response.

$K(t)$ – Control Gain

$E = diag(\varepsilon_1, \varepsilon_2)$ - is the border dense denoting the steady state error tolerance

From the Lyapunov function, it was made clear that the control gain $K(t)$ must be made sufficiently large to guarantee the global stability of the sliding mode control system. The control gain can be adjusted by following an adaptation law [13]

- If $|s| > \in > 0$, $K(t)$ is the solution of the following differential equation

  $$\dot{K}(t) = \bar{K}_1|s|,$$

  with $\bar{K}_1 > 0$ *and* $K(0) > 0$

- If $|s| < \in$, then

  $$\begin{cases} K(t) = \bar{K}_2|\rho(t)| + \bar{K}_3 \\ \tau\dot{\rho}(t) + \rho(t) = sat(E^{-1}s) \end{cases}$$

  With $\bar{K}_2 = K(t^*)$, $\bar{K}_3 > 0$ and $\tau > 0$, where t^* is the instant when $|s|$ is hitting the border $\in$.

From the first law, it is clear that the control gain $K(t)$ increases to a larger value thus overcoming the bounded parameters uncertainties and disturbances. This ensures that the $K(t)$ is larger enough to maintain the global stability of the system. The second law allows the control gain $K(t)$ to decrease and adjust according to the uncertainties and disturbances when the sliding mode starts.

The state space equation of the nonlinear system is given by (2),

$$\dot{x} = Ax + Bu + d$$

Separating out the input (u) from the above equation, we get

$$u = (\dot{x} - Ax - d)B^{-1} \tag{18}$$

From (12), we know that

$$s = x - x_{tg}$$

Differentiating this equation, with respect to time. We get

$$\dot{s} = \dot{x} - \dot{x}_{tg}$$

$$\dot{x} = \dot{s} + \dot{x}_{tg}$$

Substituting for $\dot{s}$ from (13), we get

$$\dot{x} = -\Lambda s - H\dot{s} - K(t)sat(E^{-1}s) + d + \dot{x}_{tg} \tag{19}$$

Substituting (19) in (18), we get the desired input u_{des} equation given by,

$$u_{des} = (-\Lambda s - H\dot{s} - K(t)sat(E^{-1}s) + d + \dot{x}_{tg} - Ax - d)$$

Simplifying we get,

$$u_{des} = \begin{bmatrix} \delta_\beta^{des} & M_z^{des} \end{bmatrix}^T$$

$$u_{des} = (-\Lambda s - H\dot{s} - K(t)sat(E^{-1}s) - Ax + \dot{x}_{tg})$$

The control inputs are δ_β^{des} and M_z^{des}. The δ_β^{des} is the desired front wheel steering and it is designed to constraint the vehicle side slip angle (β) within the limits. The desired external yaw moment M_z^{des} is used to track the target yaw rate r_{tg}.

A vehicle stability index based on the slip rate and turning stability index was proposed to determine the overall driving stability of the vehicle, and the proposed index was used as a weight factor that determines the intervention of the control strategy for increased efficiency and driving stability. By considering the tire force and sideslip limitation, the stability index was defined as,

$$C_{SI} = \frac{1}{2}\sqrt{\frac{\left|\beta + \omega_1\dot{\beta}\right|^2}{\beta_{limit}^2} + \frac{a_x^2 + a_y^2}{\mu^2 g^2}}$$

Where, ω_1 denotes the contribution of $\dot{\beta}$ to the instability. The control law is modified by considering both the yaw rates and side slip targets.

This modified control law is given as,

$$\begin{cases} \delta_\beta^c = \overline{sat}\left(\dfrac{C_{SI} - \xi_1}{\sigma_1}\right)\left(\delta_\beta^{des} - \delta_d\right) \\ \bar{M}_z^{des} = \overline{sat}\left(\dfrac{\xi_2 - W_\beta}{\sigma_2}\right)M_z^{des} \end{cases} \tag{10}$$

Where,

δ_β^c is the corrected steering angle for sideslip control,

ξ_i and β_i, (i=1, 2) are preselected positive constants,

$$W_\beta = \overline{sat}\left(\frac{C_{SI} - \xi_1}{\sigma_1}\right)$$

$$\overline{sat}(x) = \begin{cases} 0, & x \le 0 \\ x, & 0 < x < 1 \\ 1, & x \ge 1 \end{cases}$$

Looking at (20)**,** when the value of stability index increases, the weighting factor for M_z^{des} decreases and hence cannot be used to reduce the slip angle of the vehicle. In such cases, the front tire steering regulation is used to reduce the side slip angle by generating contra-cornering yaw moment. But, when the stability index decreases, there is no control over the sideslip angle and in such cases, the front wheel steering regulation and M_{zc} are employed to keep the sideslip angle in limits.

From the values calculated for the desired yaw rate (δ_β^C) and the desired external yaw moment (M_{zc}) from the above equations, we get a new equation for the modified yaw moment as follows,

$$\bar{M}_z^{des} = M_{zc}^{des} + 2C_f L_f \delta_{yaw}^{des}$$

Where, M_{zc}^{des} is the external yaw moment generated by the four longitudinal tire forces between two sides of the vehicle.

IV. CONTROL ALLOCATION DESIGN

In order to achieve enhanced control performance, the tracking errors of yaw rate and longitudinal acceleration must be reduced. Also, to avoid the nonlinear limit region of tire forces the control inputs need to be minimalized. Hence the cost function for the same can be defined as

$$J(v) = e^T Q e + v^T R v \tag{11}$$

In the above equation,

$$e = \begin{bmatrix} e_1 & e_2 \end{bmatrix}^T$$

$$e_1 = F_{xfl} + F_{xfr} + F_{xrl} + F_{xrr} - f_r mg - ma_x^{des}$$

$$e_2 = \frac{L_w}{2}\left(F_{xfl} - F_{xfr} + F_{xrl} - F_{xrr}\right) + 2C_f L_f \delta_{yaw}^{des} - \overline{M_z^{des}}$$

$$v = \begin{bmatrix} F_{xfl} & F_{xfr} & F_{xrl} & F_{xrr} & \delta_{yaw}^{des} \end{bmatrix}^T$$

$$Q = diag(w_{ax}, w_{yaw})$$
$$R = diag\left(\frac{w_x}{F_{zfl}^2}, \frac{w_x}{F_{zfr}^2}, \frac{w_x}{F_{zrl}^2}, \frac{w_x}{F_{zrr}^2}, w_\delta\right)$$

Where,

e_1 and e_2 are the tracking errors of yaw rate and longitudinal acceleration correspondingly,

v is a vector that denotes the actual control efforts from the actuators,

F_{zi} $(for\ i = fl, fr, rl, rr)$ is the load applied vertically on each wheel this can be calculated on each control step,

$w_{ax}, w_x, w_\delta, w_{yaw}$ are the weighting factors of tracking errors and each actuator.

These weighting factors are nothing, but functions of the stability index and they can be written as,

$$\begin{cases} w_{ax} = w_{ax0}\left[1 - \overline{sat}\left(\frac{C_{SI}}{\sigma_3}\right)\right] \\ w_{yaw} = w_{yaw0}\left[1 - \overline{sat}\left(\frac{C_{SI}}{\sigma_4}\right)\right] \\ w_x = w_{x0}\left[1 + \left(\frac{C_{SI}}{\sigma_5}\right)\right] \\ w_\delta = w_{\delta 0}\left[1 + \left(\frac{C_{SI}}{\sigma_6}\right)\right] + w_{\delta 1}W_\beta^2 \end{cases}$$

Here,

w_{ax0}, w_{yaw0}, w_{x0} and $w_{\delta 0}$ are the initial weighting factors when the stability index is zero

σ_i for i = 3, …., 6 are just some positive constants

$w_{\delta 1}$ is a large positive number chosen in such a way that when the sideslip controller is activated, the steering input for the yaw rate control can be disabled.

In reality, the actual control efforts v is constrained by tire-road adhesion limit and rate limits of the motors and hydraulic brake actuators. This can be represented as

$$\begin{cases} \frac{F_{xi}^2}{F_{zi}^2} + \frac{F_{yi}^2}{F_{zi}^2} \le \mu_i^2 \\ F_{min} \le F_{xi} \le F_{max} \\ \delta_{min} \le \delta_{yaw}^{des} \le \delta_{max} \\ F_{min}^{rt} \le F_{xi}(t + \Delta t) - F_{xi}(t) \le F_{max}^{rt} \\ \delta_{min}^{rt} \le \delta_{yaw}^{des}(t + \Delta t) - \delta_{yaw}^{des}(t) \le \delta_{max}^{rt} \end{cases}$$

Here,

μ_i is the tire friction coefficient of the i[th] tire

Δt is time step of the optimizing controller.

F_{yi} and F_{zi} are calculated using the current vehicle states at each time step

Finally, to determine the limitations of the rate limits, the constraints of the last time step are used. Therefore, the above-mentioned constraints can be shown as

$$g_j(v) \ge 0, (j = 1, \dots, 24)$$

Here the augmented Lagrangian method has been employed. This is a certain group of algorithms used to solve the constrained optimization problems. This is similar to the penalty methods, like, both replace a constrained optimization problem by a series of unconstrained problems, and they add a penalty term to the objective [14]. The difference between the two is that in augmented Lagrangian method an extra term is added that mimics the Lagrangian multiplier. But the augmented Lagrangian is different from Lagrangian multipliers. The general method for solving this assuming the constrained problem to be $\min J(v)\ such\ that\ g_j(v) \ge 0, (j = 1, \dots, 24)$. This can be solved as a series of unconstrained minimization problems. Let us first list the k[th] step of the penalty method:

$$\min \emptyset_k(x) = f(x) + \mu_k \sum_{i \epsilon I} c_i\,(x)^2$$

The penalty method can be used to solve this problem. In the next iteration the problem can resolved using a larger value of μ_k. Using the method of augmented Lagrangian function can be written as

$$\min \emptyset(v, w, \sigma_7) = J(v) + \frac{1}{2\sigma_7}\sum_{j=1}^{24}\{\left[\max\left(0, w_j - \sigma_7 g_j(v)\right)\right]^2 - w_j^2\} \quad (12)$$

here σ_7 is the penalty factor.

An updating law is used to update the multipliers $w^{(k+1)}$ in the $(k+1)^{th}$ iteration following w^k in the i[th] iteration.
The law used is:

$$w_j^{(k+1)} = \max\left\{0, w_j^k - \sigma_7 g_j(v^k)\right\} \text{ for j = 1, …, 24}$$

As we have already seen σ_i are supposed to be large positive constants. So here to update the value of σ_7 we can use the following procedure

$$h_j(v) = g_j(v) - \frac{1}{\sigma_7}\max\{0, \sigma_7 g_j(v) - w_j\}\ for\ j = 1, \dots, 24$$

$$\vartheta^k = \begin{cases} 0, & \frac{\|h(v^k)\|}{\|h(v^{(k-1)})\|} < \phi \\ 1, & \frac{\|h(v^k)\|}{\|h(v^{(k-1)})\|} \ge \phi \end{cases}$$

$$\sigma_7^{(k+1)} = \sigma_7^k + \vartheta^k(\zeta - 1)\sigma_7^k$$

where, $\phi \in (0,1)$ and $\zeta > 1$ are constant parameters.

To solve unconstrained optimization problem, the trust region method has been employed. We need to calculate the gradient vector and the Hessian matrix of $\emptyset(v, w, \sigma_7)$. For this, equation (22) can be rewritten as

$$\min \emptyset(v, w, \sigma_7) = J(v) + \frac{1}{2\sigma_7}\left[\left(w - \sigma_7 g(v)\right)^T P\left(w - \sigma_7 g(v)\right) - w^T w\right]$$

where, $P = diag(p_1, \dots, p_{24})$ can be calculated in each of the iteration using

$$p_j^k = \begin{cases} 0, & w_j^k - \sigma_7 g(v^k) \le 0 \\ 1, & w_j^k - \sigma_7 g(v^k) > 0 \end{cases} \qquad j = 1, \dots, 24$$

V. SIMULATION

In the paper all simulations are done using a software called CarSim. But due to our constraints regarding accessing the software, alternately we have used MATLAB and Simulink to simulate the controller.

In the paper, for simulation of the entire model in CarSim they have considered various other parameters like,

- Initial velocity of the vehicle = 50km.h^{-1}
- The tire friction coefficient = 0.5
- The desired longitudinal acceleration = 2.5m.s^{-2}
- At 2s there was an anticlockwise turn made that caused the hand wheel steering angle to be at 3.5 degrees.
- The yaw rate needs a θ which is kept at 0.15.

Fig. 4a and 4c show the vehicle yaw rates and accelerations with respect to time respectively. For the intended steering input and longitudinal acceleration from the driver, the desired yaw rate had grown bigger than the upper bound, i.e. $r_{des} > r_{limit}$. The controlled longitudinal acceleration was maintained at 2.0 ms^{-2} and it was observed that as the vehicle speed kept increasing the value of r_{limit} kept decreasing, this is shown in Fig 4a. There was a comparison made with the system having the controller for the above parameters and one without the controller. It was observed that the yaw rate when the controller is present follows the reference perfectly, while the yaw rate without the controller shows large understeer which can be seen in Fig 4d. Thus, we understand that a controlled vehicle will follow the desired trajectory while the vehicle without the controller had deviated from the desired curve due to severe understeer. It was noticed that a_x and $\sum \frac{F_{xi}^2}{F_{zi}^2}$ $for\ i = fl, fr, rl, and\ rr$ for a controlled vehicle are directly related to the w_{ax} and w_x terms in the cost function. The relation observed is that when w_x increases the value of $\sum \frac{F_{xi}^2}{F_{zi}^2}$ decreases, as a result of this the vehicle slip decreases. But also, this leads to a decrease in $\sum F_{xi}$ which further leads to a decrease of a_x by 0.5m.s^{-2} as can be observed from Fig 4c.

Whereas, in a controlled vehicle the lateral acceleration stabilized at 3.8m.s^{-2} which results in the planar acceleration to be 4.3m.s^{-2}. This is 0.86 times μg, and this implicates that the vehicle was around the critical condition, but the longitudinal and lateral slips were still in the stable regions. It can be observed from Fig 4b that the vehicle sideslip angle finally settled down at about 2.9 degrees and both the longitudinal and lateral tire sideslip angle were constrained in the stable region and avoiding large sideslip or spinning which is shown in Fig 5 and 6. In case of a vehicle without the controller, the vehicle sideslip was lesser than the one with the controller but the longitudinal sideslip ratio and the sideslip angle of the front tires were much larger than the rear tires. Further, the longitudinal slip ratio of the front left tire kept increasing with oscillations leading to serious understeer of the vehicle.

It was understood from Fig 7 that the stability index of the controlled vehicle was not larger than the threshold ξ_1 in the simulations, and thus only the steering control was used for the generation of yaw moment M_z. Also, the tire forces on the outer were much larger than that on the inner side.

It is noticed from Fig 8 that the yaw moment M_{zc} in the direction of the steering was generated to release the demand of the steering angle. Attached below are the graphs of the same.

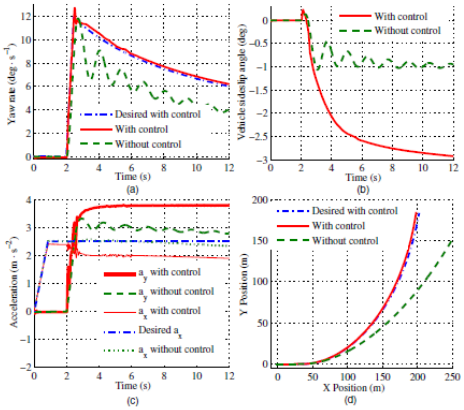

Fig. 4. Vehicle body response in the simulation

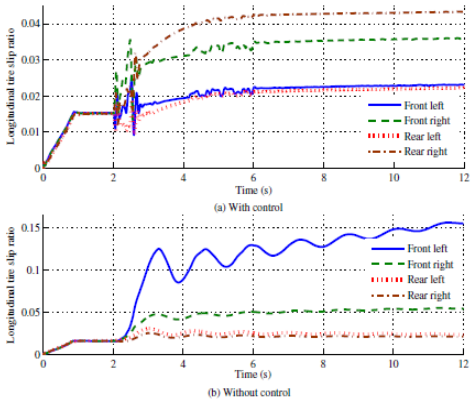

Fig. 5. Longitudinal tire slip ratio in the simulation

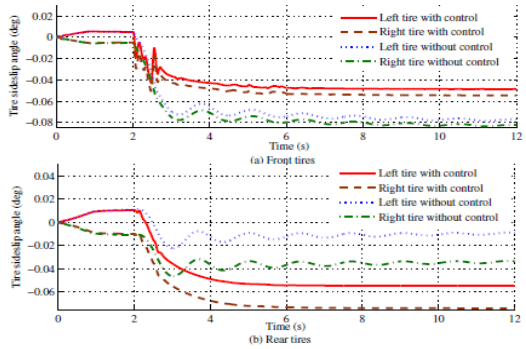

Fig. 6. Side slip angle in the simulation

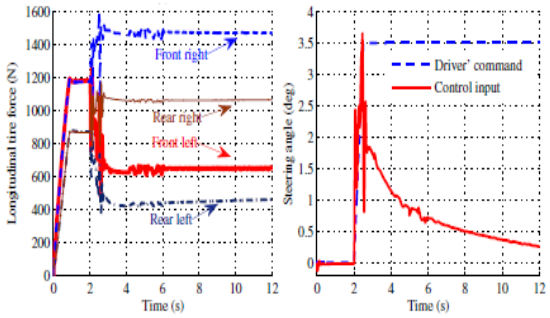

Fig. 7. Controller input to the simulation

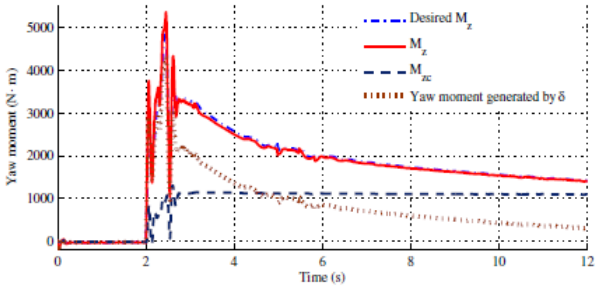

Fig. 8. Yaw moment in the simulation

For our simulation purposes we gave a step signal as the input to our controller which we have shown in Fig. 9. We checked the output by varying various parameters like Gain (K), the convergence of error (λ) and layer thickness (E).

First, we fixed the thickness at 0.01, λ at 5 and K at 10, but there were overshoots and the output later stabilizes. Next, we maintained the thickness at 0.01, λ at 5 and varied K. After changing K to 20 the output seemed to stabilize around 2s. Since, K(t) is the control gain of the controller, the value of it must be kept high to ensure stability of the controller according to the Lyapunov's function [13]. But, maintaining the gain of the controller to be very high is practically not possible. Hence, an optimum value of K(t) = 20 is chosen for the controller. We further tried to check the output by maintaining the same K and thickness and decreasing the λ to 1. When this change was made the output seemed to stabilize but much slower. It stabilized only around 6s. Then we kept the K at 20 as it is and changed λ back to 5 and then increased the thickness to 1. It was observed that the output again had overshoots and later stabilizes. Finally, we maintained K at 20 and the thickness at 0.01 and increased λ to 10. It was observed that the overshoots increased.

Hence, we found that the most optimum values for the controller at which it stabilizes quickly are when K is at 20 and λ is at 5 and thickness is 0.01. The coordination weighting law transfers the priority between tracking desired yaw motion and maintaining stability according to the change of vehicle states. Fig. 15 shows the switching response of the controller based on the input parameters we provided to get the desired output response. Looking at Fig.11 and Fig.15, the switching phenomenon happens only till the output is stabilised i.e., at 2s, till the output follows the input signal. While simulating, we do not consider the constraints by tire-road adhesion limit and rate limits of the motors and hydraulic brake actuators. Hence, there is not much chattering after the system is stabilised. But, in real time nonlinear systems there will be more switching and more chattering occurring even after the system is stabilised. In this paper, they have shown a control allocation algorithm using Lagrangian multipliers to account for the chattering phenomenon due to the constraints in a real system. The below figures show these output graphs. The blue lines in the graphs show the inputs and the red lines depict the outputs.

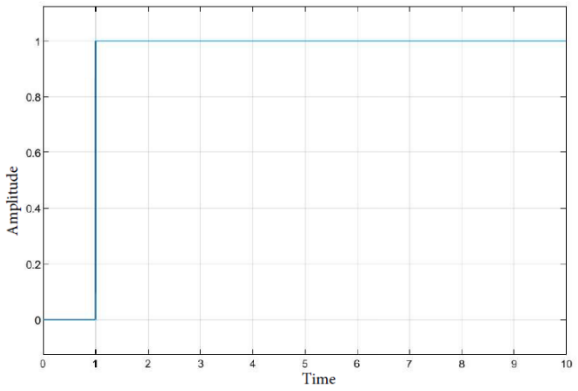

Fig. 9. Input step signal to the controller

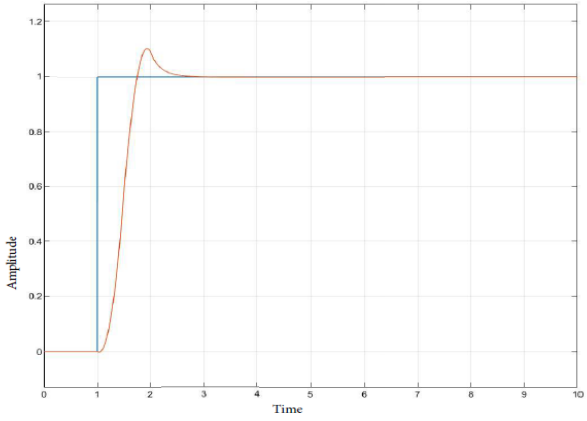

Fig. 10. Output Response with K = 10, λ = 5 and E = 0.01

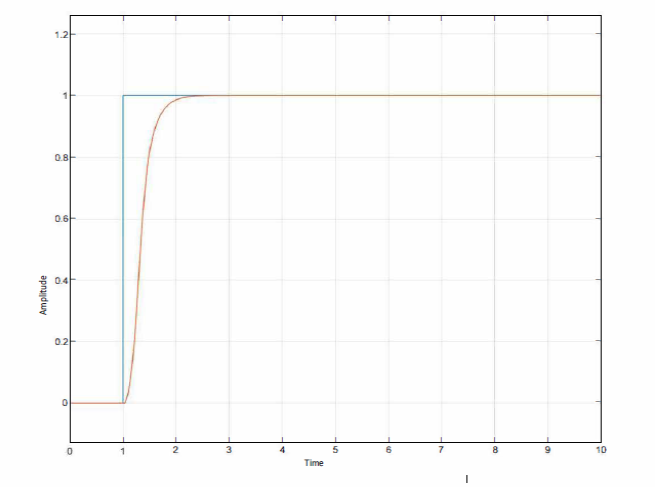

Fig. 11. Output Response with K = 20, λ = 5 and E = 0.01

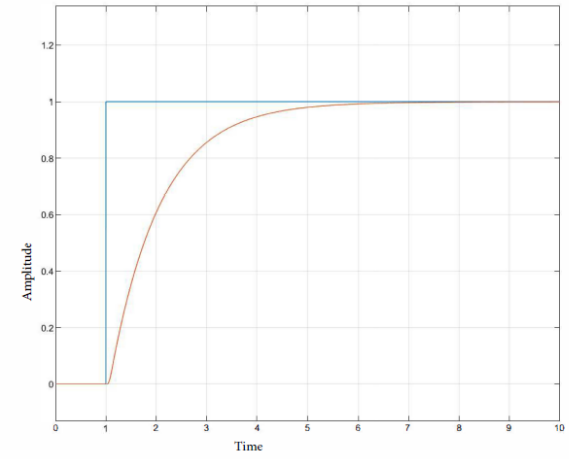

Fig. 12. Output Response with K = 20, λ = 1 and E = 0.01

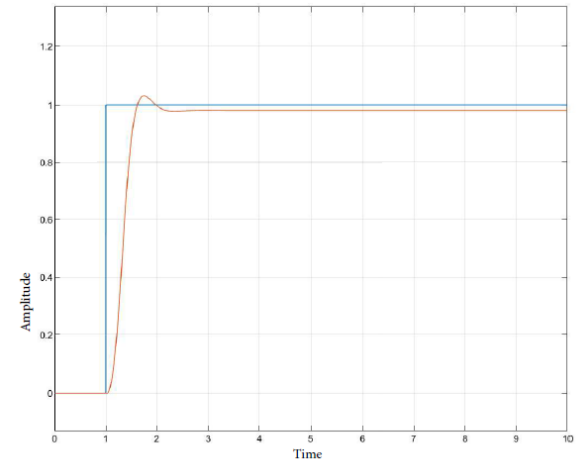

Fig. 13. Output Response with K = 20, λ = 5 and E = 1

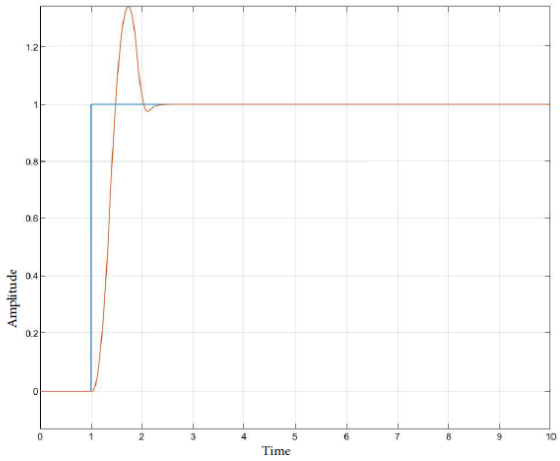

Fig. 13. Output Response with K = 20, λ = 10 and E = 0.01

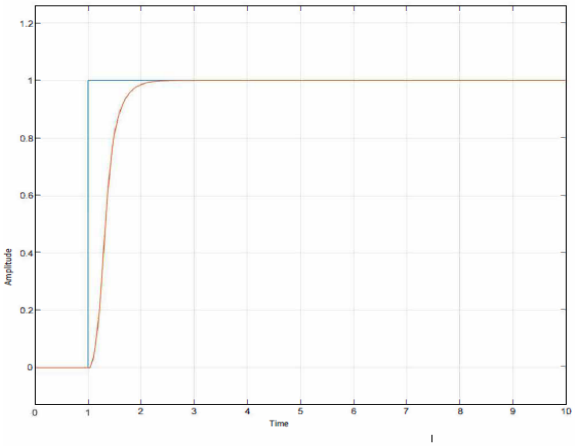

Fig. 14. Desired output Response with K = 20, λ = 5 and E = 0.01

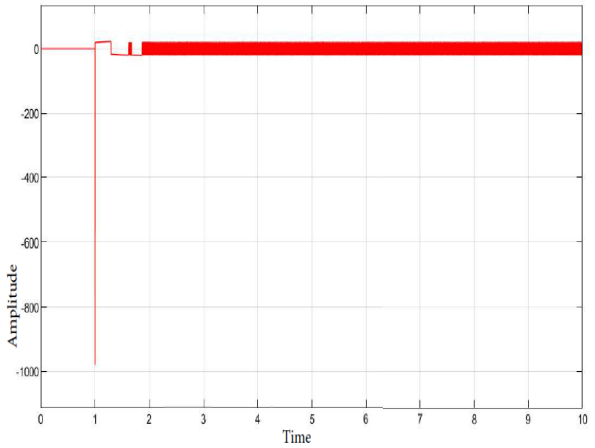

Fig. 15. Switching characteristics with desired output response

VI. CONCLUSION

In this paper, the desired front wheel steering angle and the corrective yaw moment is determined keeping the side slip angle of the vehicle well below the tolerable limits by considering the vehicle stability index. This is done by using an adaptive sliding mode controller as the higher-level controller. The stability of the vehicle is given higher priority over the input yaw motion angle from the steering input. Thus, the coordination weighting law transfers the priority between tracking desired yaw motion and maintaining stability according to the change of vehicle states. It was also noted that the sliding mode controller responded well against the low sensitivity to the plant parameter uncertainty and provided an added advantage of finite time convergence which exists because of the discontinuous control law. Noted downside of adaptive sliding mode controllers includes the high chattering due to the implementation imperfections and the over focus of the controller on the matched uncertainties (i.e., uncertainties that enter the control channel).

In reality, the actual control efforts are constrained by tire-road adhesion limit and rate limits of the motors and hydraulic brake actuators. Hence, a lower level controller, a control allocation algorithm with actuator and tire force considerations was designed to assign the desired yaw moment calculated from the higher level controller to the front wheel steering system and four wheels In the control allocation, the weighting factors of the tracking errors and control inputs in the cost function are updated online according to the vehicle stability index. Simulation results show that the overall performance of handling and stability is well improved by tracking desired yaw rate and maintaining reasonable sideslip.

REFERENCES

[1] Wang, J., Wang, R., Jing, H. and Chen, N. (2015). "*Coordinated Active Steering and Four-Wheel Independently Driving/Braking Control with Control Allocation. American Control Conference"*, 18(1), pp.5420-5425.

[2] R. Wang, Y. Chen, D. Feng, X. Huang, and J. Wang, "*Development and performance characterization of an electric ground vehicle with independently actuated in-wheel motors*," Journal of Power Sources, vol. 196, no. 8, pp. 3962-3971, 2011.

[3] A Goodarzi, E. Esmailzadeh IEEE/ASME Trans. Mech., 12 (6) (2007), pp. 632-639

[4] R. Wang, J. Wang Proceedings of the 2010 ASME Dynamic Systems and Control Conference (2010)

[5] J. Wang, R. Longoria IEEE Trans. Control Systems Technol., 17 (3) (2009), pp. 723-732

[6] T. Gordon, M. Howell, and F. Brandao. "*Integrated control methodologies for road vehicles*," Vehicle System Dynamics, vol. 40, nos. 1-3, pp. 157-190, 2003.

[7] R. P. Osborn and T. Shim, "*Independent control of all-wheel-drive torque distribution*," Vehicle System Dynamics, vol. 44, no. 7, pp. 529-546, 2006.

[8] En.wikipedia.org. (2019). *Active steering*. [online] Available at: https://en.wikipedia.org/wiki/Active_steering [Accessed 30 Oct. 2019].

[9] En.wikipedia.org. (2019). *Sliding mode control*. [online] Available at: https://en.wikipedia.org/wiki/Sliding_mode_control [Accessed 6 Nov. 2019].

[10] J. Ackermann, "Robust control prevents car skidding," IEEE Control Systems, vol. 17, no. 3, pp. 23-31, 1997.

[11] A. T. Van Zanten, R. Erhardt, and G. Pfaff, "*VDC, the vehicle dynamics control system of Bosch*," SAE Technical Paper, no. 950759, 1995.

[12] En.wikipedia.org. (2019). Lyapunov stability. [online] Available at: https://en.wikipedia.org/wiki/Lyapunov_stability [Accessed 24 Nov. 2019].

[13] V. I. Utkin, A. S. Poznyak, *"Adaptive Sliding Mode Control*," *Advances in Sliding Mode Control*, Springer Berlin Heidelberg, pp. 21- 53, 2013.

[14] En.wikipedia.org. (2019). *Augmented Lagrangain method*. [online] Available at: https://en.wikipedia.org/wiki/Augmented_Lagrangian [Accessed 24 Nov. 2019].

[15] Mathworks.com. (2019). *Example on Sliding Mode Control - File Exchange - MATLAB Central*. [online] Available at: https://www.mathworks.com/matlabcentral/fileexchange/52429-example-on-sliding-mode-control [Accessed 25 Nov. 2019].

APPENDIX

Abbreviations

VTD	Variable Torque Distribution
BFD	Brake Force Distribution
AWS	Active Front Wheel Steering

Notations

δ_f	Front Wheel Steering angle
δ_s	Conventional Steering angle
δ_c	Additive Steering angle from controller
I_z	Vehicle Inertia along z axis
r	Yaw rate
β	Vehicle side slip angle
C_f	Front tire cornering stiffness
C_r	Rear tire cornering stiffness
d_1 and d_2	External disturbances
M_{zc}	Generated external yaw moment
l_s	Track width
δ	Front wheel steering angle
$G_{ss}(V_x)$	Steady state Gain
r_{des}	Desired yaw rate
δ_d	Desired steering angle
a_y	Lateral acceleration
a_x	Longitudinal acceleration
V_x	Velocity component in x axis
V_y	Velocity component in y axis
θ	Positive constant
g	Gravity
r_{des}	Desired yaw rate
r_{limit}	Limit
s	Sliding mode suface
r_{tg}	Vehicle yaw rate reference
β_{tg}	Vehicle slip angle reference
V	Lyapunov Function
Λ	Converge speed of s
H	Reduces overshoot of tracking response
$K(t)$	Control Gain
$E = diag(\varepsilon_1, \varepsilon_2)$	Steady state error tolerance
u_{des}	Desired Control input
δ_β^{des}	Desired front wheel angle constraining (β)
M_z^{des}	Desired external yaw moment
C_{SI}	Stability Index
ξ_i and β_i	Preselected positive constants
$J(v)$	Cost function of the system
e_1	Tracking error of yaw rate
e_2	Tracking error of longitudinal acceleration
v	Vector denoting force efforts from actuator
F_{zi} $(for\ i = fl, fr, rl, rr)$	Load applied vertically on each wheel this can be calculated on each control step
$w_{ax}, w_x, w_\delta, w_{yaw}$	Weighting factors of tracking errors and each actuator
w_{ax0}, w_{yaw0}, w_{x0} and $w_{\delta 0}$	Initial weighting factors when the stability index is zero
σ_i for i = 3, …., 6	Positive constants
$w_{\delta 1}$	Large positive number input for disabling yaw rate control

μ_i	Tire friction coefficient of the i^{th} tire
Δt	Time step of the controller
F_{yi} and F_{zi}	Calculated using the current vehicle states at each time step
σ_7	Penalty factor
$\phi \in (0,1)$ and $\zeta > 1$	Constant parameters